Behavior of Bidirectional Spring Unit in Isolated Floor Systems

Shenlei Cui, M.ASCE[1]; Michel Bruneau, F.ASCE[2]; and Amarnath Kasalanati, P.E.[3]

Abstract: To investigate the mechanical behavior of bidirectional spring units used as isolators in a kind of isolated floor system, three types of characterization tests were conducted—from spring components alone to the complete spring unit in its implemented configuration. The test results show that the behavior of the springs and spring units is stable when subjected to cyclic repeated motions, and is not sensitive to the velocity of motion. The hysteretic behavior of the spring units was found to be unconventional, with bilinear and different ascending (loading) and descending (unloading) branches. Based on the experimental behavior, a physical model was developed to replicate the unique behavior of such bidirectional spring units. Good agreement was found from the comparison between the results from the physical model and the corresponding tests. Finally, a sensitivity study, with respect to the model's four primary defining parameters, shows that this physical model is more sensitive to the sliding friction coefficient between the spring cable and the bushing in the spring unit than to the other three parameters.

DOI: 10.1061/(ASCE)ST.1943-541X.0000187

CE Database subject headings: Structural engineering; Seismic design; Earthquakes; Isolation; Models; Floors.

Author keywords: Structural engineering; Seismic design; Earthquake; Isolation; Models; Floor isolation; Spring unit.

Introduction

Extensive research has been conducted in the past decades to develop and implement technologies (such as lead-elastomer bearings and friction pendulum bearings) for the seismic base isolation of buildings [e.g., Naeim and Kelly (1999) and Fenz and Constantinou (2008), to name a few]. In recent years, there has been a growing interest in isolating only the specific equipment or specific floors of buildings. Isolating equipment rather than entire buildings can be challenging to some types of isolation devices due to the relatively low mass supported by the isolators. Various systems have been developed to isolate equipment, such as ball-in-cone isolators [Kemeny and Szidarovszky (1995) and Kasalanati et al. (1997) to name a few] and another system studied by Fathali and Filiatrault (2007). These isolation systems generally focused on the response of the equipment isolated.

Floor isolation systems have been implemented in Japan for over 15 years. Complex mechanisms are used (Takase et al. 1997) to provide three-dimensional isolation by using gravity based systems (suspension mechanisms) or linear spring based systems (coil springs or rubber units used for restoration force), with viscous dampers or lead plugs used for damping. Kaneko et al. (1995) reported that a floor isolated system in Kansai area worked effectively during the 1995 Hyogoken-Nanbu Earthquake.

In the United States, isolated floor systems are gaining interest in various applications to protect nonstructural components that can be moved and located anywhere on the floor or specific rooms—instead of isolating single equipment or the entire building. One such type of system uses a special kind of bidirectional spring units to provide stiffness, damping and self-centering capabilities to the isolated floor. This system is a physical substitute of a raised floor (or a computer access floor) and is designed to protect the contents in computer data centers with minimal intrusion of retrofit.

To investigate the force-displacement behavior of these unique bidirectional spring units, characterization tests were conducted on the springs alone as well as on the overall system. A physical model that captures the unique behavior of the bidirectional spring units was developed and its predictions were compared to the experimental results. Finally, a sensitivity study of this physical model with respect to its four primary parameters is presented.

Description of Bidirectional Spring Unit

An image of the bidirectional spring unit and a conceptual sketch of its application in isolated floor system are shown in Figs. 1(a and b). The isolated floor is supported on casters (rollers), which provide the vertical load transfer with unimpeded horizontal movement in any direction. A steel cable connects the isolated floor and the bidirectional spring unit, which is mounted on (or attached to) the nonisolated ground/floor. Owing to the placement of the spring under the isolated floor, any horizontal movement of the isolated floor results in vertical pull of the cable, which causes extension in the spring. The extension of the spring provides the restoring force for the isolated floor. Fig. 2 compares the input motion applied on the shake table (representative of what

[1]Graduate Research Assistant, Dept. of Civil, Structural and Environmental Engineering, State Univ. of New York at Buffalo, Buffalo, NY 14260 (corresponding author).

[2]Professor, Dept. of Civil, Structural and Environmental Engineering, State Univ. of New York at Buffalo, Buffalo, NY 14260.

[3]Director of Engineering, Dynamic Isolation Systems, Inc., Sparks, NV 89434.

Note. This manuscript was submitted on December 2, 2008; approved on January 9, 2010; published online on January 13, 2010. Discussion period open until January 1, 2011; separate discussions must be submitted for individual papers. This paper is part of the ***Journal of Structural Engineering***, Vol. 136, No. 8, August 1, 2010. ©ASCE, ISSN 0733-9445/2010/8-944–952/$25.00.

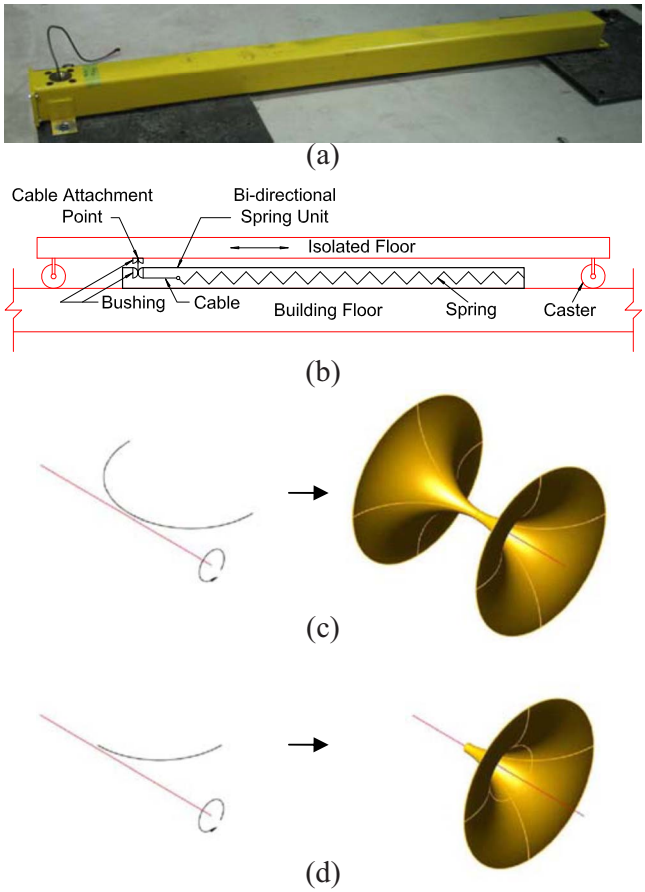

Fig. 1. Bidirectional spring unit: (a) overview; (b) application in isolated floor system; (c) revolution of semicircle; and (d) revolution of quarter circle

the contents of a nonisolated floor would experience) with the motion of the isolated floor. As seen here, the isolated floor reduces the accelerations by 50 to 75%, demonstrating effective behavior of the system. [For more details on this, see Cui and Bruneau (2010).]

The steel cable that connects the isolated floor and the spring passes through a bushing. The main purpose of this bushing is to provide smooth curvature from a horizontal spring to the vertical contact with the isolated floor. The bushing is capable of accommodating 180° rotation of the cable in vertical plane and 360° rotation in horizontal plane. The surface of this bushing is the revolution of a semicircle around an external axis parallel to the diameter as shown in Fig. 1(c). The sliding of the cable on the bushing results in significant damping, which is discussed in detail in the later sections. Another bushing at the underside of the isolated floor accommodates rotations up to 90° vertically and 360° horizontally, thus allowing the isolated floor to move horizontally without bending the cable at connection point. Note that there is no sliding between this bushing and the steel cable (due to the fixed vertical connection point). The surface of this bushing is a revolution of a quarter circle around an external axis as shown in Fig. 1(d). Looking from above, the bushing surface looks like the inside surface of the flare of a "trumpet." The bushing in the spring unit (where sliding occurs) is made of brass, and the one on the isolated floor (where no sliding occurs) is made of steel.

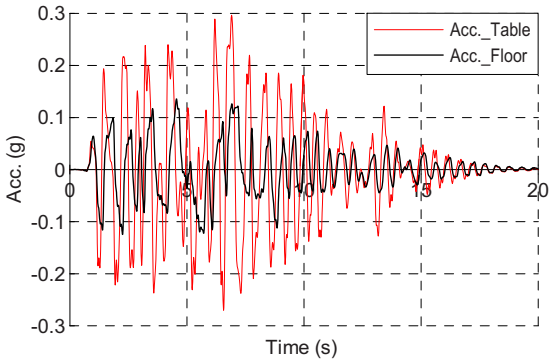

Fig. 2. Performance of the isolated floor system: comparison of shake-table accelerations (input) and accelerations on top of the isolated floor

Characterization Tests

Specimen Setup and Instrumentation

Three types of tests were conducted to determine the force-displacement relationship of the spring unit as a complete component, as well as that of its internal individual spring, namely,

1. Test Series 1: axial tests of individual springs left within the tube, without threading the cable through the bushing of the spring unit, to investigate the behavior of the spring alone;
2. Test Series 2: axial tests of individual springs taken out of the tube but resting on a steel channel at the same height level corresponding to the bottom surface of the tube in Test Series 1, to capture the behavior of the spring alone and compare results with those from Test Series 1, in an attempt to quantify friction between the spring and the tube. Under this new setup, the spring could be openly seen, unlike the Test Series 1 tests where the spring was hidden by the tube;
3. Test Series 3: tests of complete spring unit assembly, in same configuration as implemented in the corresponding isolated floor system.

Results from Test Series 1 and 2 showed that the spring, sagging downward due to its self-weight, was always in contact with the bottom of the tube during its motion. This friction results in a small hysteresis as described in the "Results" section. Note that for Test Series 1 and 2, the spring, load cell, and actuator were aligned on the same axis.

The specimen setup for Test Series 1 to 3 is shown in Fig. 3. For Test Series 3, to simulate the working conditions of the spring units as they are installed in the complete isolated floor system, an anchor end was manufactured to hold the spring cable. A bushing was welded to the bottom plate of the anchor end to simulate the bushing on the isolated floor shown in Fig. 1(b). In the specimen setup for this series of tests shown in Fig. 3(c), note that the central lines of the load cell and the actuator shaft were arranged such that the clear distance between the bushing on the anchor end and the bushing in the spring unit was set to be 20 mm (0.783 in) to simulate the working condition of the spring unit in complete isolated floor system.

Input Program

To check whether the behavior of the individual spring and spring unit is sensitive to cyclic repeated motions and velocity, sinusoidal displacement input of ten cycles with different frequen-

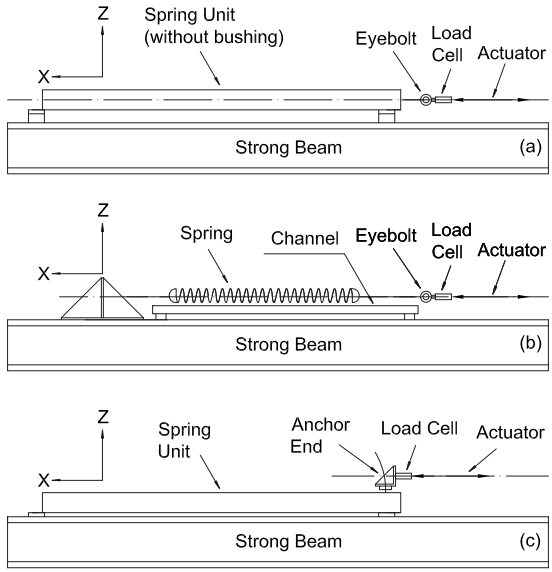

Fig. 3. Specimen configurations: (a) Test Series 1; (b) Test Series 2; and (c) Test Series 3

cies were used during these characterization tests. Sinusoidal displacement signals of amplitude of 254 and 203 mm at a frequency of 0.05 and 0.2 Hz, respectively, were used. For those amplitudes of the sinusoidal signals, the velocity at each point of the 0.2 Hz sine wave was 3.2 times that of the corresponding 0.05 Hz wave.

Some seismic floor displacement inputs were also adopted as inputs to test the bidirectional spring units. These are relative displacement histories between the isolated floor and the base floor recorded during the tests of an isolated floor system using this kind of bidirectional spring units. They are called 2Acc31wo, 3Acc31wo, B107050, and B207050, and are considered to reflect a representative range of floor response histories, as shown in Fig. 4.

Half-sinusoidal input was used for Test Series 1 and 2 because the spring is tested alone in these and can only be pulled. For the same reasons, the seismic floor displacement histories were not used for these two test series. For Test Series 3, the complete "pull" and "push" parts of the sinusoidal signals and the seismic displacement records were used.

Test Protocol

Bidirectional spring units can be built with internal springs having different stiffnesses to meet the design needs of the isolated floor systems. Springs with two different nominal stiffnesses were considered as part of the current test program. Also, to investigate consistency between nominal (specified) and actual stiffness within a group, *two* springs with nominal stiffness of 2,627 N/m (15 lb/in), and *two* springs with nominal stiffness of 1,313 N/m (7.5 lb/in) were tested. A total of 36 tests were conducted on the spring units for the three series of tests. The names of tests were chosen per the following nomenclature:

1. Names for sinusoidal inputs consist of *five* parts from left to right: (1) Signal frequency (0.05 Hz is expressed as "05," and 0.2 Hz as "2"); (2) Pretension, noted as null ("0") or 51 mm (2 inches expressed as "2"); (3) Nominal spring stiffness (15 lb/in is expressed as "15" and 7.5 lb/in as "07"); (4) Presence of the tube, noted as with ("w") or without ("wo"); and (5) Presence of the bushing noted as with ("w") or without ("wo").

   For example, "05150wowo" means test for a 0.05 Hz sinusoidal input signal, for a spring of 2,627 N/m (15 lb/in) nominal stiffness spring, without pretension, and without tube and bushing on (i.e., Test Series 2). For Test Series 1 and 2, only one spring of each nominal stiffness was tested. For Test Series 3, two springs of each nominal stiffness were assembled and tested sequentially to check the repeatability of the behavior of the spring units. In Test Series 3, there is an extra "2" at the end of the names of the tests to denote that the second spring of same nominal stiffness was used.
2. Names of tests using seismic floor displacement record inputs are constructed using seismic displacement record input name, followed by the same conversion indicated above for the nominal spring stiffness, the pretension condition (null or 51 mm), and whether the tests was conducted with or without tube, and with or without bushing.

Results of Test Series 1 and 2

Figs. 5 and 6 show the results of the spring tests without pretension and with 51 mm (2 in) pretension when subjected to different frequency sinusoidal motions, respectively. Note that parts (a) and (b) in each of these figures are not in the same vertical axes scale. As shown in these figures, the behavior of the individual spring is stable under cyclic repeated motions. Also, note that the force-displacement loops corresponding to different frequency sinusoidal motions agree well with each other, demonstrating that the behavior of the springs is not sensitive to motion frequency/velocity. In addition, note that the results from Test Series 1 (spring in the tube, no bushing) and those from Test Series 2

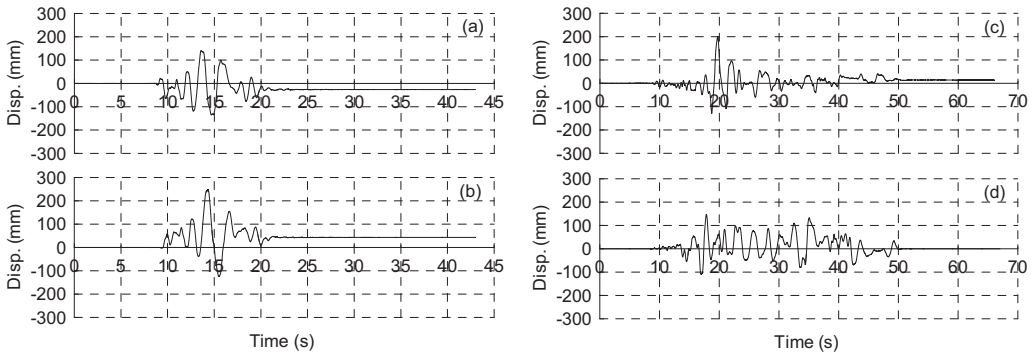

Fig. 4. Seismic displacement histories: (a) 2Acc31wo; (b) 3Acc31wo; (c) B107050; and (d) B207050

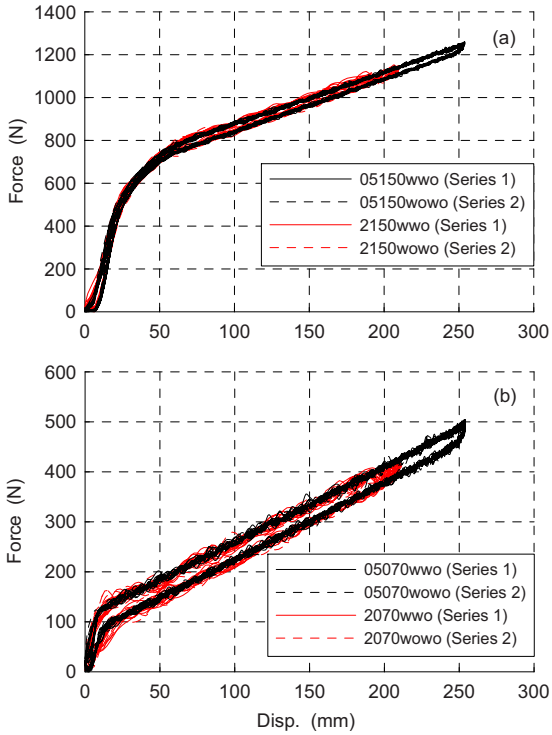

Fig. 5. Results of Test Series 1 and 2—spring tests without pretension: (a) 2,627 N/m spring; (b) 1,313 N/m spring

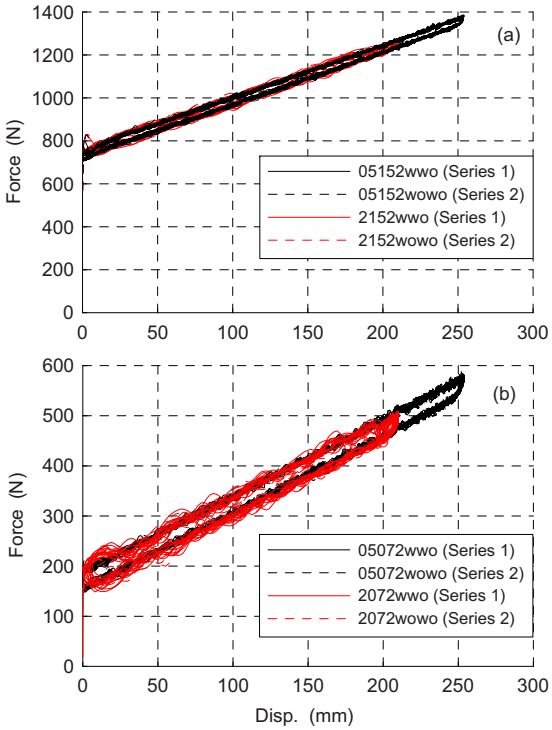

Fig. 6. Results of Test Series 1 and 2—spring tests with 51 mm pretension: (a) 2,627 N/m spring; (b) 1,313 N/m spring

(spring on steel channel, no bushing) overlay perfectly on top of each other, confirming that the configurations of Test Series 1 and 2 are actually identical.

From Fig. 5(a), note that for the 2,627 N/m (15 lb/in) nominal stiffness spring without any pretension, the behavior is bilinear with a small offset at the beginning, or trilinear if a small linear segment is used to model the offset. The first phase of behavior is relatively soft when the displacement is less than about 6 mm (0.25 in), then much stiffer until a displacement of about 51 mm (2 in), after which elongation proceeds per a lower linear stiffness of about 2,428 N/m (13.9 lb/in). Note that the springs are designated with this secondary stiffness (specified values of 15 lb/in and tested value of 13.9 lb/in in this case). From Fig. 5(b), it is found for the 1,313 N/m (7.5 lb/in) nominal stiffness spring without any pretension that the behavior is bilinear. After a displacement of about 10 mm (0.4 in), the spring starts to elongate with a linear stiffness of about 1,525 N/m (8.7 lb/in). When the springs were pretensioned by 51 mm (2 in) before starting the tests, as shown in Fig. 6, the curves plotted starting from zero displacement were linear. These pretensioned curves corresponded to the data that would be read from the curves shown in Fig. 5 if starting to read the curves from a point that is 51 mm (2 in) right of the ordinate axis. Figs. 5 and 6 also show that each of the force-displacement curves obtained for the spring components exhibit some small hysteresis around the mean force line. This hysteresis is likely attributed to the friction between the spring and the tube in Test Series 1 and between the spring and the steel channel in Test Series 2, the value of which is around 18 N (4 lb).

Results of Test Series 3

Complete spring units were tested without and with pretension, for sinusoidal motions and earthquake displacement records. Fig. 7 shows the results of complete spring unit tests without any pretension. The results of tests with 51 mm (2 in) pretension are illustrated in Fig. 8. Note that parts (a) and (b) in each of these figures are not in the same vertical axes scale. From these figures, note that the force-displacement loops, when subjected to cyclic sinusoidal motions, agree well with each other from test to test

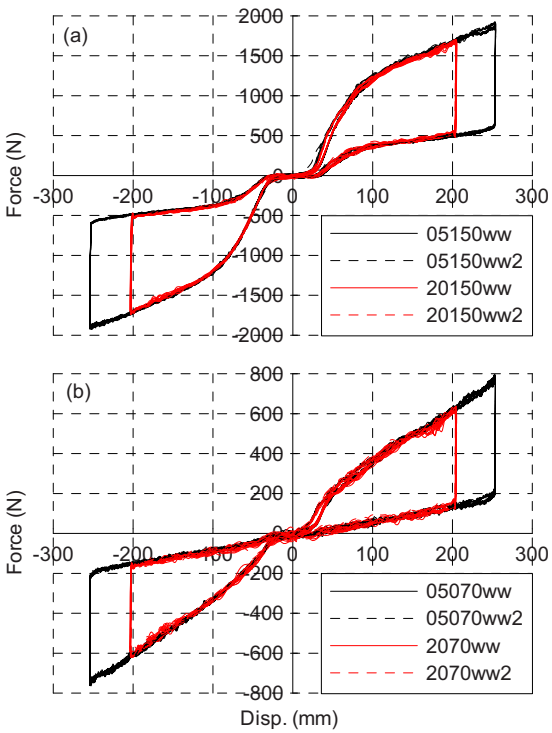

Fig. 7. Results of Test Series 3—spring unit tests without pretension: (a) 2,627 N/m spring unit; (b) 1,313 N/m spring unit

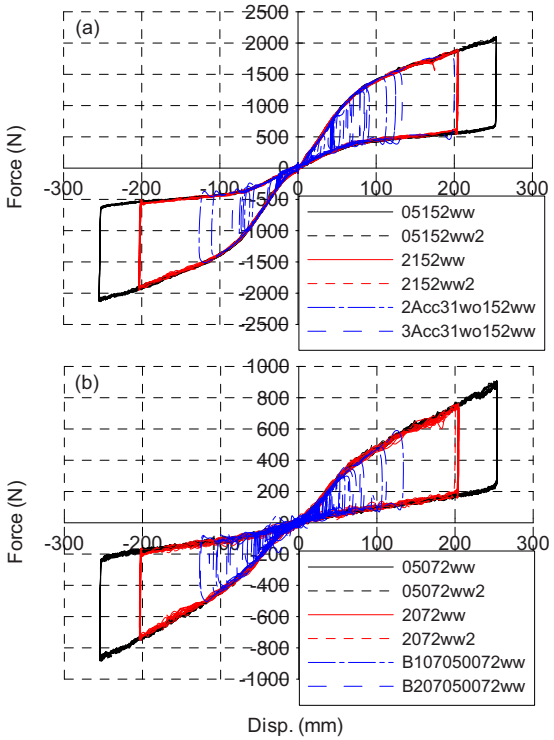

Fig. 8. Results of Test Series 3—spring unit tests with 51 mm pretension (a) 2,627 N/m spring unit; (b) 1,313 N/m spring unit

and that the behavior of the spring unit is stable under cyclic repeated motion. Further, the behavior of the spring units is also stable with respect to the frequencies/velocities of motions. Fig. 8 also demonstrates that the behavior of the spring unit subjected to seismic displacement records coincide well with the corresponding ones subjected to sinusoidal signals, which again confirms that the hysteretic behavior of the spring units is stable and not sensitive to displacement history. Figs. 7 and 8 also show consistency in the force-displacement loops for both spring units with same nominal stiffness. However, the shape of the hysteretic loop itself is unconventional and needs further explanation. The physics of this behavior is described in next section. The lateral force (F)-lateral displacement (D) curve goes up bilinearly when loading, drops vertically on load reversal, and goes down a different bilinear path when unloading. The F-D curve transitions to a linear stiffness for the loading and unloading branches at a displacement of 76 mm (3 in) for the system with 2,627 N/m (15 lb/in) spring and 30 mm (1.2 in) for the system with 1,313 N/m (7.5 lb/in) spring. However, the unloading slopes are different from the loading slopes, as explained in the next section.

Physical Model

The detailed geometric relationships, needed to develop the physical model for unidirectional floor motions, take into account both the bushing in the spring unit and the bushing fixed on the underside of the isolated floor, and are shown in Fig. 9. In this figure, "$F_1 \pm f$" is the force in the spring cable at the end which connects to the internal spring in the spring unit, "r" is the radius of each of the two bushings, which is 31 mm (1.218 in) for the case at hand, "β" is the angle over which the spring cable is in contact with the bushing and "θ" is the complementary angle of "β," "Δ" is the horizontal relative displacement between the isolated floor and the spring unit underneath, and "a" is the clear distance between the bushings [which is 20 mm (0.783 in) as mentioned before]. The total floor displacement, Δ, can be divided into geometric dimensions "$b+2c$" and "$2d$," which are the horizontal projections of the cable segments between the bushings that are not in contact and in contact, respectively, with the quarter circle segments of the bushings. "F_3" is the horizontal restoring force of the spring unit corresponding to the isolated floor displacement (Δ). Note that the spring cable is simplified as a line without thickness for simplicity.

For the horizontal travel distance Δ, shown on Fig. 9 as equal to $b+2(c+d)$, the following geometric relationship during motion can be obtained, knowing that $b=a/\tan\theta$, $c=r(1-\cos\theta)/\tan\theta$, and $d=r(1-\sin\theta)$

$$\Delta = a/\tan\theta + 2r[1 - \sin\theta + (1 - \cos\theta)/\tan\theta] \quad (1)$$

As shown in Fig. 9, $\beta=\pi/2-\theta$. Substituting, the above relationship may be expressed as

$$\Delta = a\tan\beta + 2r[1 - \cos\beta + (1 - \sin\beta)\tan\beta] \quad (2)$$

Substituting $\beta=2\alpha$ allows simplifying the resulting expression knowing that

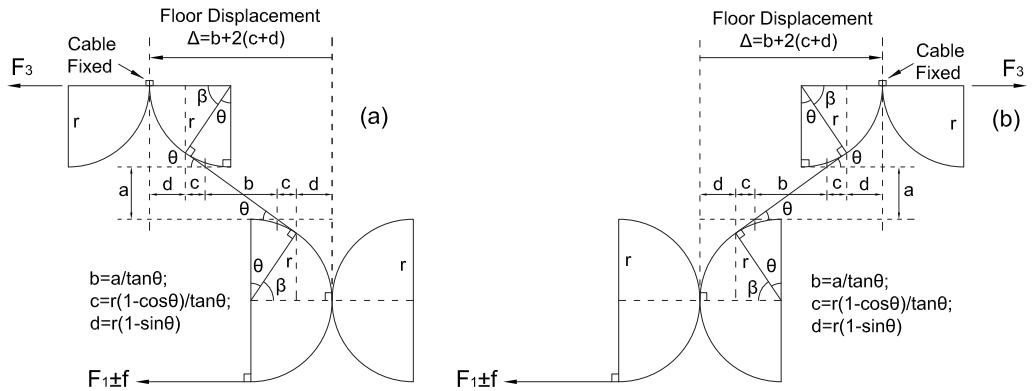

Fig. 9. Geometry of bushing and cable system during floor motion: (a) floor motion toward the spring unit; (b) floor motion away from the spring unit

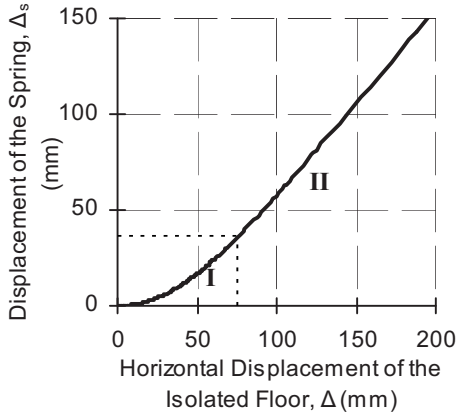

Fig. 10. Relationship between the spring extension and horizontal floor displacement

$$\sin\beta = \frac{2\tan\alpha}{1+\tan^2\alpha}, \quad \cos\beta = \frac{1-\tan^2\alpha}{1+\tan^2\alpha}, \quad \text{and} \quad \tan\beta = \frac{2\tan\alpha}{1-\tan^2\alpha} \tag{3}$$

Substituting these into Eq. (2), and substituting $\tan\alpha$ by x (to simplify the resulting expression) gives the following equation:

$$(\Delta - 4r)x^2 + 2(a+2r)x - \Delta = 0 \tag{4}$$

Solving Eq. (4) gives

$$x = \frac{-(a+2r) \pm \sqrt{(a+2r)^2 + \Delta(\Delta-4r)}}{\Delta - 4r} \text{ (when } \Delta \neq 4r) \tag{5}$$

From calculation and comparison with bushing motion geometry, for the positive value of x

$$x = \frac{-(a+2r) + \sqrt{(a+2r)^2 + \Delta(\Delta-4r)}}{\Delta - 4r} \text{ (when } \Delta \neq 4r) \tag{6}$$

Because $\beta = 2\alpha$ and $x = \tan\alpha$, then

$$\beta = 2a\tan\left[\frac{-(a+2r) + \sqrt{(a+2r)^2 + \Delta(\Delta-4r)}}{\Delta - 4r}\right] \text{ (when } \Delta \neq 4r) \tag{7}$$

Note that when $\Delta = 4r$, Eq. (7) converges to $\beta = 1.296$.

From Fig. 9, the elongation the internal spring of the bidirectional spring unit, denoted as Δ_s here, corresponding to the isolated floor horizontal displacement, Δ, can be expressed as

$$\Delta_s = a/\cos\beta + 2r\beta + 2r(1-\sin\beta)/\cos\beta - 2r - a \tag{8}$$

Hysteretic Behavior Model for Pretensioned Bidirectional Spring Units

Fig. 10 shows the relationship between Δ_s and Δ. Physically, there are two distinct regions of movement: (1) the wrapping of the cable around the quarter circles of the bushing in the early part of the movement, resulting in increase in the contact angle (i.e., β in Fig. 9), and (2) steady pulling of the spring at larger displacements when the quarter circles are nearly fully wrapped, during which the contact angle (i.e., β in Fig. 9) is near to 90°. In both regions of movement, there is sliding between the cable and the bushing. In the first region of movement (i.e., zone I in Fig. 10), there is a rapid increase in force, attributed mainly to the increase in the contact angle. This is seen as a region of high initial stiffness in the *F-D* curve. In the second region of movement (i.e., zone II in Fig. 10), the angle of contact is nearly constant and as a result, the slope is linear in the *F-D* curve.

Considering bidirectional spring units in isolated floor system will be pretensioned by prepulling the cable by 51 mm (2 in) to facilitate self-centering of the system, here, the physical model of bidirectional spring units considering pretension was first developed. The linear force-displacement relationships of pure springs (within tube) with 51 mm (2 in) pretension, shown in Fig. 6, can be simulated with straight lines for the average force ("F_1" in Fig. 9, treated as pure spring force) and a small hysteretic friction ("f" in Fig. 9) to capture the observed friction effect.

For the 2,627 N/m (15 lb/in) spring with 51 mm (2 in) pretension case, the equation of the straight line used to simulate the average force (F_1)-displacement (Δ_s) relationship, in units of N and mm respectively, is

$$F_1 = 2.428\Delta_s + 745.481 \tag{9}$$

For the 1,313 N/m (7.5 lb/in) spring with 51 mm (2 in) pretension case, the equation of the line used to model the pure spring force (F_1)-displacement (Δ_s) relationship, in units of N and mm respectively, is

$$F_1 = 1.525\Delta_s + 169.198 \tag{10}$$

As mentioned above, the friction, f, is around 18 N (4 lb). Therefore, the force-displacement relationships of springs (in tube) with 51 mm (2 in) pretension are equal to the corresponding straight lines plus and minus the friction effect when the cable is extending out and retracting in, respectively.

Then, based on the belt friction formula (Bedford and Fowler 2005), the force in the spring cable segment outside the bushing, denoted as F_2, can be expressed as

$$F_2 = (F_1 + f)e^{\mu_k(\pi/2+\beta)} \text{ (when the cable is extending out)} \tag{11}$$

$$F_2 = (F_1 - f)/e^{\mu_k(\pi/2+\beta)} \text{ (when the cable is retracting in)} \tag{12}$$

The horizontal restoring force F_3, equal to the horizontal component of F_2, can be obtained as following:

$$F_3 = (F_1 + f)e^{\mu_k(\pi/2+\beta)}\cos\theta \text{ (extension)} \tag{13}$$

$$F_3 = (F_1 - f)/e^{\mu_k(\pi/2+\beta)}\cos\theta \text{ (retraction)} \tag{14}$$

where μ_k = sliding friction coefficient (which is a kinetic friction coefficient) between the steel cable and the brass bushing. No values of kinetic friction coefficient could be found for these two materials under greasy contacting surface. Sliding friction coefficient values of μ_k of 0.171 and 0.190 were found to be adequate for the 2,627 N/m (15 lb/in) and 1,313 N/m (7.5 lb/in) nominal stiffness spring units, respectively. These values of the sliding friction coefficient are evaluated statistically to give the minimum sum of square error comparing the model prediction and the corresponding test result.

In all the equations shown above, the displacement and force parameters are treated as scalars, that is, these parameters have no vector directional meaning. Therefore, in computations, if the force and displacement are defined as positive in one motion direction, then the force and displacement in the opposite direction should be considered with a negative sign. Note that four key physical terms were used in developing this model: r, a, f, and μ_k are the physical properties of the spring unit itself and are denoted

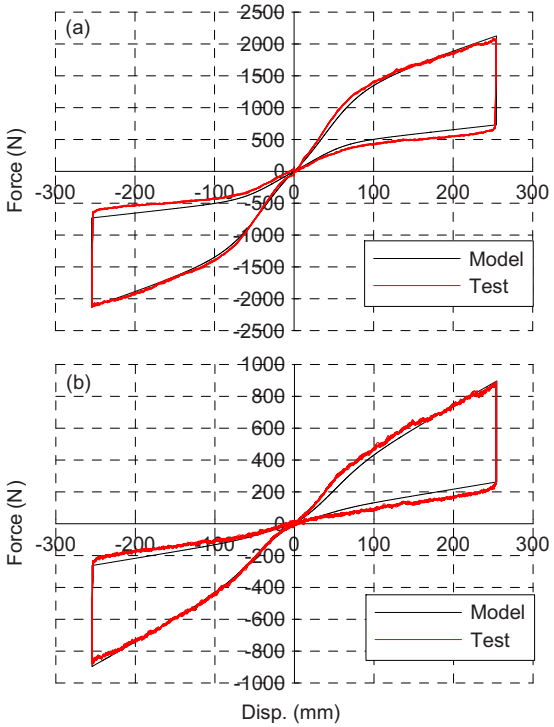

Fig. 11. Comparison of results between model and corresponding test: (a) 2,627 N/m spring unit (test of 05152ww); (b) 1,313 N/m spring unit (test of 05072ww)

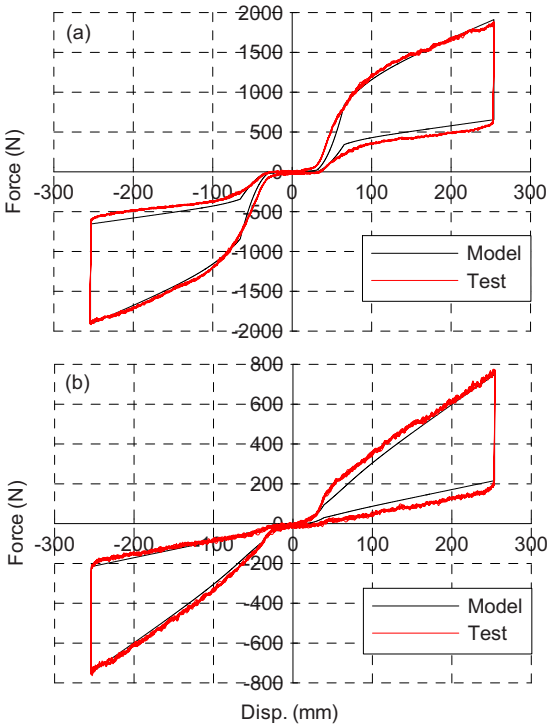

Fig. 12. Comparison of results from model and corresponding test: (a) 2,627 N/m spring unit (test of 05150ww); (b) 1,313 N/m spring unit (test of 05070ww)

as primary parameters, using which all the other quantities (i.e., β, Δ_s, F_1, F_2, and F_3) can directly or indirectly be expressed

Hysteretic Behavior Model for Non-Pretensioned Bidirectional Spring Units

The above process can also be used for the development of the physical analytical model for bidirectional spring units *without* any pretension and with a different amount of pretension as long as the corresponding values of the four primary parameters and the force-displacement relationship of spring components are known. As an example, the following will show the development of the physical model for bidirectional spring units *without* pretension using these equations shown above. The only difference of this process is that the force-displacement relationships [i.e., Eqs. (9) and (10)] must be replaced by the corresponding force-displacement relationship of springs without any pretension. The values of the four primary parameters (r, a, f, and μ_k) are kept same as those used in model for pretension cases.

For the 2,627 N/m (15 lb/in) spring without any pretension case, a trilinear model was adopted here. The equations of the lines in different displacement phases used to simulate the pure spring force (F_1)-displacement (Δ_s) relationship, in units of N and mm respectively, are

$$F_1 = 2.643\Delta_s + 2.802 \text{ (when } \Delta_s \leqslant 6.3 \text{ mm)} \quad (15)$$

$$F_1 = 31.363\Delta_s + 179.117 \text{ (when } 6.3 \text{ mm} < \Delta_s \leqslant 27.6 \text{ mm)} \quad (16)$$

$$F_1 = 2.429\Delta_s + 618.606 \text{ (when } \Delta_s > 27.6 \text{ mm)} \quad (17)$$

For the 1,313 N/m (7.5 lb/in) spring without any pretension case, a bilinear model was adopted here. The equations of the lines in different displacement phases used to simulate the pure spring force (F_1)-displacement (Δ_s) relationship, in units of N and mm respectively, are

$$F_1 = 9.598\Delta_s + 7.704 \text{ (when } \Delta_s \leqslant 10.1 \text{ mm)} \quad (18)$$

$$F_1 = 1.514\Delta_s + 88.947 \text{ (when } \Delta_s > 10.1 \text{ mm)} \quad (19)$$

The comparison of results from model and the corresponding characterization tests for both with and without pretension cases are presented in the following section.

Comparison between Test and Physical Model

The comparisons of the model prediction and the corresponding experimental results for tests 05152ww and 05072ww are shown in Fig. 11 for the case of pretensioned spring units. The model predicts well the initial phase (rapid rise in force) and the secondary phase of the loading and unloading branches. The comparisons of the model and the corresponding experimental results for tests of 05150ww and 05070ww for nonpretension cases are shown in Fig. 12. Again, the model predicts well the trilinear nature of these results.

Sensitivity Study of Physical Model

For a given spring stiffness and pretension, the physical model developed was defined in terms of four primary parameters: r, a, f, and μ_k. To investigate how variation in the values of these parameters influences this physical model's ability to capture the behavior of the spring units, a sensitivity study was conducted.

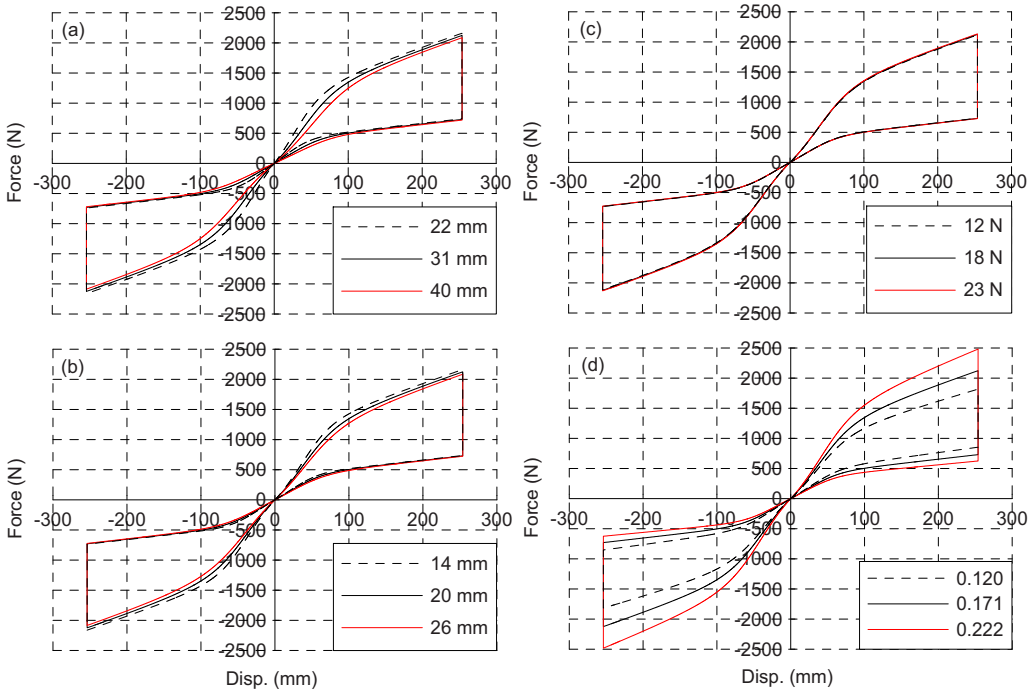

Fig. 13. Results of sensitivity study: (a) with respect to r; (b) with respect to a; (c) with respect to f; and (d) with respect to μ_k

Analyzes were sequentially conducted on the four primary parameters mentioned above by separately using values 30% larger and smaller than that of each parameter in the physical model. As an example, the resulting bidirectional spring unit hysteretic behavior obtained from this sensitivity study are shown in Fig. 13 for the 2,627 N/m spring unit with 51 mm (2 in) pretension. Similar results and trends were observed for the softer spring units (Cui and Bruneau 2010).

From Figs. 13(a and b), note that a 30% change of r or a does not result in a significant difference in behavior. When increasing the value of r or a by 30%, the initial stiffness (for both loading and unloading branches) of the hysteretic curve respectively decreases on average by 15 and 9% (and similarly increase for decreasing values of r or a). However, the secondary stiffness practically remains unchanged. Furthermore, the maximum force decreases by less than 3% for a 30% increase of either r or a. Fig. 13(c) shows that the physical model is not sensitive to a 30% variation of f, as the corresponding hysteretic curves practically coincide with each other. The physical model is, however, more sensitive to variations in sliding friction coefficient (μ_k). Significant difference in behavior (i.e., force value difference at same displacement) can be found from Fig. 13(d). Note that the hysteretic curve expands when μ_k increases. For example, for a 30% increase in μ_k, the initial and secondary stiffnesses of the loading branch of the hysteretic curve correspondingly increase by 13% and 18% on average, and the maximum force developed in this case increases by 17%. For the unloading branch of the hysteretic curve, the trends observed above are reversed. However, the transition point between the two different stiffnesses in each branch practically remains at the same displacement.

It is important to recognize that this isolation system controls the movement of the floor in the horizontal direction. It does not provide isolation in the vertical direction. However, except at ground levels where the vertical acceleration of the earthquake would be directly felt on a slab-on-grade foundation, on most floors, the vertical acceleration of the earthquake will be attenuated by the vibration frequencies of the beams supporting the floors. While this could be an interesting problem which received little attention in the past, it has not been shown to be a major issue in past earthquakes. If the vertical accelerations were of concern, this isolation system will have to be modified to accommodate this in some way, which is beyond the scope of this research. Note that most existing base isolation systems, for equipment or even for structures, similarly do not address vertical excitations.

Conclusions

To investigate the behavior of the individual springs and the complete bidirectional spring units, three series of characterization tests were conducted. The test results show that the behavior of the springs and the spring units is stable when subjected to cyclic repeated motions, and is not sensitive to motion velocity. The hysteretic behavior of the spring units was found to be unconventional but fully explainable from mechanics, with bilinear and different ascending (loading) and descending (unloading) branches. Based on the experimentally obtained behavior, a physical model was developed to simulate the unique behavior of such kind of bidirectional spring units. Comparison of results from the physical model and corresponding characterization test shows good agreement. A sensitivity study of this physical model with respect to the four physical parameters characterizing the bidirectional spring unit shows that the physical model developed here is more sensitive to variations in the sliding friction coefficient between the spring cable and the bushing in the spring unit than to the other three parameters. This physical model provides a foundation to simulate the behavior of the complete isolated floor system using this kind of bidirectional spring units in the future.

Future Research Needs

The purpose of this paper was to develop a physical model for engineers to better understand the fundamental behavior of a floor isolated using special spring units of the type considered here. While this is an important and necessary building block to understand the behavior of this isolated floor system during real earthquake excitations, it does not, by itself, provide predictions of the behavior of the complete isolated floor system during such events. Therefore, there is a need for extensive series of tests on such systems under shake-table excitations, that will allow to investigate the behavior under various conditions as expressed by other sets of parameters (such as pretension level, spring units having different stiffnesses, unidirectional earthquake excitation, bidirectional earthquake excitation, variation of floor response spectra characteristics, and others). Furthermore, this would allow investigating possible limitations in applicability of this system, as well as the importance of the quality of construction during erection of this system.

Acknowledgments

This work was supported in whole by the Earthquake Engineering Research Centers Program of the National Science Foundation under Award No. ECC-9701471 to the Multidisciplinary Center for Earthquake Engineering Research. The bidirectional spring unit is a proprietary device patented by Dynamic Isolation Systems, Inc. (DIS). The floor isolation system and the springs were provided by DIS for this study. Any opinions, findings, conclusions, and recommendations presented in this paper are those of the writers and do not necessarily reflect the views of the sponsors.

References

Bedford, A., and Fowler, W. T. (2005). *Engineering mechanics statics*, Pearson Education, Inc., Upper Saddle River, N.J., 488–490.

Cui, S., and Bruneau, M. (2010). "Development of integrated design methodology for selected isolated floor systems in single-degree-of-freedom structural fuse systems." *Rep. No. MCEER-10–0005*, Multidisciplinary Center for Earthquake Engineering Research, Univ. at Buffalo, State Univ. of New York, Buffalo, N.Y.

Fathali, S., and Filiatrault, A. (2007). "Experimental seismic performance evaluation of isolation/restraint systems for mechanical equipment. Part I: Heavy equipment study." *Report No. MCEER-07–0007*, Multidisciplinary Center for Earthquake Engineering Research, Univ. at Buffalo, State Univ. of New York, Buffalo, N.Y.

Fenz, D., and Constantinou, M. C. (2008). "Spherical sliding isolation bearings with adaptive behavior: Theory." *Earthquake Eng. Struct. Dyn.*, 37(2), 163–183.

Kaneko, M., Yasui, Y., and Okuda, Y. (1995). "Simultaneous horizontal and vertical vibration tests of three-dimensional floor isolation system." *AIJ J. Technol. Des.*, 1, 186–190.

Kasalanati, A., Reinhorn, A., Constantinou, M. C., and Sanders, D. (1997). "Experimental study of ball-in-cone isolation system." *Building to Last: Proc., Structures Congress XV*, ASCE, Reston, Va., 1191–1195.

Kemeny, Z. A., and Szidarovszky, F. (1995). "Seismic isolation bearings with nonlinear gravity restoring." *Report No. MCEER VF01127*, Multidisciplinary Center for Earthquake Engineering Research, Univ. at Buffalo, State Univ. of New York, Buffalo, N.Y.

Naeim, F., and Kelly, J. M. (1999). *Design of seismic isolated structures*, Wiley, New York.

Takase, N., Arima, F., Tanaka, H., and Egasira, H. (1997). "Development of three-dimensional floor-isolated system. Part I: Dynamic characteristics of floor-isolated method by suspended structure (SNR-F system)." *Summaries of technical papers of Annual Meeting Architectural Institute of Japan. B-2, Structures II, Structural dynamics nuclear power plants*, 595-596 (in Japanese).